Process Safety and Environmental Protection 218 (2026) 109520

Contents lists available at ScienceDirect

Process Safety and Environmental Protection

journal homepage: www.journals.elsevier.com/process-safety-and-environmental-protection

Insights into sludge reduction in a sequencing batch reactor integrated with an anaerobic side-stream reactor

Muhammad Fauzul Imron[a,b,*], Lenno van den Berg[c], Alexander Hendriks[c], Ralph E.F. Lindeboom[b], Merle de Kreuk[b]

[a] Study Program of Environmental Engineering, Department of Biology, Faculty of Science and Technology, Universitas Airlangga, Kampus C UNAIR, Jalan Mulyorejo, Surabaya 60115, Indonesia
[b] Department of Water Management, Faculty of Civil Engineering and Geosciences, Delft University of Technology, Stevinweg 1, Delft 2628CN, the Netherlands
[c] Haskoning, Laan 1914 no 35, Amersfoort 3818EX, the Netherlands

ARTICLE INFO

Keywords:
Anaerobic side-stream reactor
In situ sludge reduction
Phosphate release
Sequencing batch reactor
Wastewater treatment

ABSTRACT

Sludge production remains a major challenge in wastewater treatment and integrating an anaerobic side-stream reactor (ASSR) into the return activated sludge line is a promising technology for in situ sludge reduction. Thus, this research investigates the performance and internal mechanisms of an ASSR integrated with a sequencing batch reactor (SBR) under prolonged side-stream retention conditions for in situ sludge reduction. The results showed that this configuration reduced the observed sludge yield by 42% (0.288 → 0.166 g VSS/g COD), while maintaining stable COD removal of 85–90%. Ammonium removal remained high, although nitrate accumulation during part of the operation indicated that nitrogen conversion was not fully stable. Total phosphorus (TP) removal reached up to 98% during early operation, accompanied by phosphate release in the ASSR of up to 250 mg PO_4^{3-}-P/L, indicating the formation of a phosphate-rich side-stream. However, TP removal and phosphate release declined during later operation, showing that this response was not sustained throughout the experiment. A simplified flow-based VSS balance indicated that the net VSS difference across the ASSR was equivalent to approximately 25% of the difference in sludge production between the two systems. Endpoint microbial profiles and predicted functional profiles differed among the reactors and were consistent with community differentiation under the integrated operating conditions. However, they did not establish the active metabolic pathways. Overall, the lower system-wide observed sludge yield reflected the combined effects of solids transformation in the ASSR, longer biomass retention, and repeated anaerobic–aerobic exposure.

1. Introduction

The generation of sludge is one of the major issues in the operation of wastewater treatment plants (WWTPs). Worldwide, WWTPs produce large quantities of sludge at around 0.05–0.10 kg dry solids/person/d (Gao et al., 2020). In European countries, the annual sludge production is on average 8.7 million tons of dry solid waste (EurEau, 2021), with treatment and disposal costs ranging from 75 to 100 € per ton of dewatered sludge (STOWA, 2024). The large volume of sludge generated significantly increases operational costs up to 20–30% and can cause environmental problems if not managed properly (Ferrentino et al., 2016). Reducing sludge production through cost-effective and efficient technologies remains a critical research priority to lower operational expenses and minimize environmental impacts.

Physical and chemical methods in WWTPs have been applied extensively for in situ sludge reduction, including ozonation, chlorination, and thermochemical treatments to promote the disintegration of sludge structures (Ferrentino et al., 2023; Sun et al., 2022). Nevertheless, the impact of these technologies can also be caused by side effects, such as high cost, formation of residues or by-products, and may inhibit biological processes (Patel et al., 2021). One of the promising alternatives for in situ sludge reduction that does not require high operational cost is the application of an anaerobic side-stream reactor (ASSR) in the return activated sludge line (Ferrentino et al., 2021; Peng et al., 2023). In this configuration, settled activated sludge is recirculated through an anaerobic tank before returning to the aerobic tank (Cheng et al., 2022).

* Corresponding author at: Study Program of Environmental Engineering, Department of Biology, Faculty of Science and Technology, Universitas Airlangga, Kampus C UNAIR, Jalan Mulyorejo, Surabaya 60115, Indonesia.
E-mail addresses: M.F.Imron@tudelft.nl, fauzul.imron@fst.unair.ac.id (M.F. Imron).

https://doi.org/10.1016/j.psep.2026.109520
Received 11 June 2026; Received in revised form 11 August 2026; Accepted 26 August 2026
Available online 27 August 2026

The alternation between aerobic and anaerobic conditions, combined with extended sludge retention times (SRT) and exposure to a broader range of redox conditions, promotes mechanisms such as metabolic uncoupling, where a fraction of the substrate is oxidized for cellular maintenance rather than biomass growth, cell lysis, extracellular polymeric substances (EPS) degradation, and the enrichment of slow-growing bacteria, all of which contribute to reduced observed sludge yield (Semblante et al., 2014). Although this configuration shares operational similarities with side-stream enhanced biological phosphorus removal (S2EBPR), the objectives are fundamentally different (Morello et al., 2024a). S2EBPR primarily applies short-term anaerobic exposure to enrich polyphosphate-accumulating organisms (PAOs) and improve phosphorus removal (Zhang et al., 2023), whereas ASSR is mainly designed to induce sludge minimization through prolonged anaerobic biomass transformation (Cheng et al., 2022).

Several previous studies have focused on the application of ASSR combined with discontinuous-flow or continuous-flow fed activated sludge and demonstrated that this integration can minimize sludge production while maintaining the performance of the primary wastewater treatment technology. Huang et al. (2019) reported that the lowest observed sludge yield was obtained when the sequencing batch reactor (SBR) was complemented with an ASSR (0.292 g TSS/g COD), with a sludge reduction efficiency up to 38% compared to the control SBR (0.473 g TSS/g COD). Morello et al. (2024b) reported that the combination of a membrane bioreactor and an ASSR reduced sludge production by 38–48%, with a hydraulic retention time (HRT) of 6–24 h in the ASSR. Moreover, Zhao et al. (2021) claimed that the ASSR can induce phosphate release through hydrolysis of polyphosphate (poly-P) by PAO under anaerobic conditions, providing avenues for phosphorus recovery. These studies indicate that ASSR integration can influence both sludge production and nutrient transformation. However, most previous studies have primarily emphasized overall observed sludge yield reduction, while less attention has been given to how sludge minimization is linked with internal sludge transformation in the ASSR, phosphate release dynamics, microbial community shifts, and operational stability. In particular, the consequences of extended anaerobic side-stream exposure for EPS transformation, phosphate release stability, and sludge settleability require further investigation.

Therefore, this study evaluated an SBR–ASSR system operated at a nominal ASSR SRT of 10 d by addressing three research questions: (1) Does the integration of an ASSR reduce the observed sludge yield relative to a control SBR while maintaining wastewater treatment performance? (2) How large is the net VSS change across the ASSR relative to the difference in sludge production between the two systems? (3) How does repeated exposure to the ASSR affect phosphorus dynamics, sludge settleability, particle characteristics, and microbial community structure? Together, these questions provide a basis for distinguishing solids transformation within the ASSR from broader system-level effects and for evaluating the operational trade-offs of the integrated configuration.

2. Materials and methods

2.1. Synthetic wastewater

Synthetic domestic wastewater was prepared with pollutant concentrations based on the influent characteristics of the Harnaschpolder WWTP, Den Hoorn, the Netherlands. The recipe was adapted from Gonzalez et al. (2021) (Table S1). The feed solution was prepared in tap water by mixing carbon, nitrogen, and phosphorus sources, along with macro- and micronutrients. The characteristics of the prepared synthetic wastewater are shown in Table 1. These values were representative of typical domestic wastewater in terms of organic matter and nutrient content in the Harnaschpolder WWTP, Den Hoorn, the Netherlands (Guo et al., 2020b). The total phosphorus (TP) fraction included both organic and particulate forms, most likely originating from milk powder and egg white powder, as well as dissolved inorganic phosphate.

Table 1
Characteristics of synthetic domestic wastewater.

Parameters	Value (mg/L, except ratios and pH)
tCOD	450 ± 64
sCOD	75 ± 2.5
VFA (as acetate)	34 ± 0.5
BOD_5	201 ± 18
Ratio BOD_5/tCOD	0.45 ± 0.02
TN	74 ± 8.70
NH_4^+-N	43 ± 16
NO_2^--N	0.007 ± 0.00
NO_3^--N	1.55 ± 0.75
TP	9.36 ± 0.36
PO_4^{3-}-P	2.44 ± 0.89
TS	1410 ± 24
VS	462 ± 17
TSS	380 ± 28
VSS	260 ± 28
VSS/TSS	0.7 ± 0.13
pH	8 ± 0.1

2.2. Experimental setup and operational conditions

Two laboratory-scale treatment systems (Fig. 1) were used in this experiment: (i) an SBR as the control (SBR.C) and (ii) an SBR (main reactor, SBR.M) coupled to an ASSR. Prior to the experimental phase, both systems were seeded and acclimated. Aerobic sludge (~5 g/L) from the Harnaschpolder WWTP, Den Hoorn, the Netherlands, was used to seed the SBR. The ASSR was inoculated with waste-activated sludge (~10 g/L) originating from the same WWTP but previously conditioned in a semi-continuous thermophilic sludge pre-treatment, continuously stirred reactor operated under anaerobic conditions at 55°C with HRT 5.5 h as described by Monteiro et al. (2026). The conditioned sludge was selected to facilitate the initial establishment of hydrolytic and fermentative activity under the anaerobic conditions of the ASSR in order to shorten the start-up phase. After that, all the systems were acclimated for approximately 90 d until chemical oxygen demand (COD) removal stabilized, defined as no significant difference between two consecutive measurements.

Both SBRs had a working volume of 4 L and were operated in 4 h cycles, corresponding to six cycles per day. The influent and effluent flow rates for the SBR were both 8 L/d (~1333 mL/cycle), an HRT of 12 h in each SBR or an exchange of 1/3 of the volume per cycle. Each cycle included 10 min of filling, 50 min of anaerobic phase, 60 min of aerobic phase, and 45 min of anoxic phase, followed by 60 min of settling, 10 min of decanting, and 5 min of idling. In SBR.C, a target SRT of 10 d was maintained by withdrawing settled sludge twice weekly, while the calculated effective SRT was approximately 15 d. In the integrated SBR.M–ASSR system, sludge was continuously exchanged between the two reactors. Therefore, the effective SRT was calculated for the combined system and was approximately 46 d. Despite this difference in whole-system SRT, both SBRs were operated at the same COD loading rate of 0.2 kg COD/kg DS/d and at comparable MLSS concentrations. Sludge was exchanged between SBR.M and the ASSR once per cycle. During the idling phase of the SBR.M cycle, 200 mL/d (~33 mL/cycle) of settled sludge was transferred from the SBR to the ASSR. Subsequently, during the feeding phase of the SBR.M, an equal volume of mixed liquor was returned from the ASSR to the SBR. The 2 L ASSR volume was determined from the applied sludge-interchange rate of 200 mL/d and the target nominal side-stream retention time of 10 d. The resulting ASSR-to-SBR volume ratio of 0.5 was therefore a consequence of the selected experimental retention and interchange conditions rather than a proposed full-scale design ratio. When the ASSR volume was included, the integrated SBR.M–ASSR configuration had a nominal total liquid-volume-to-influent-flow ratio of 18 h. However, the ASSR received no direct wastewater influent and was connected to SBR.M only through internal sludge exchange. The oxidation-reduction potential

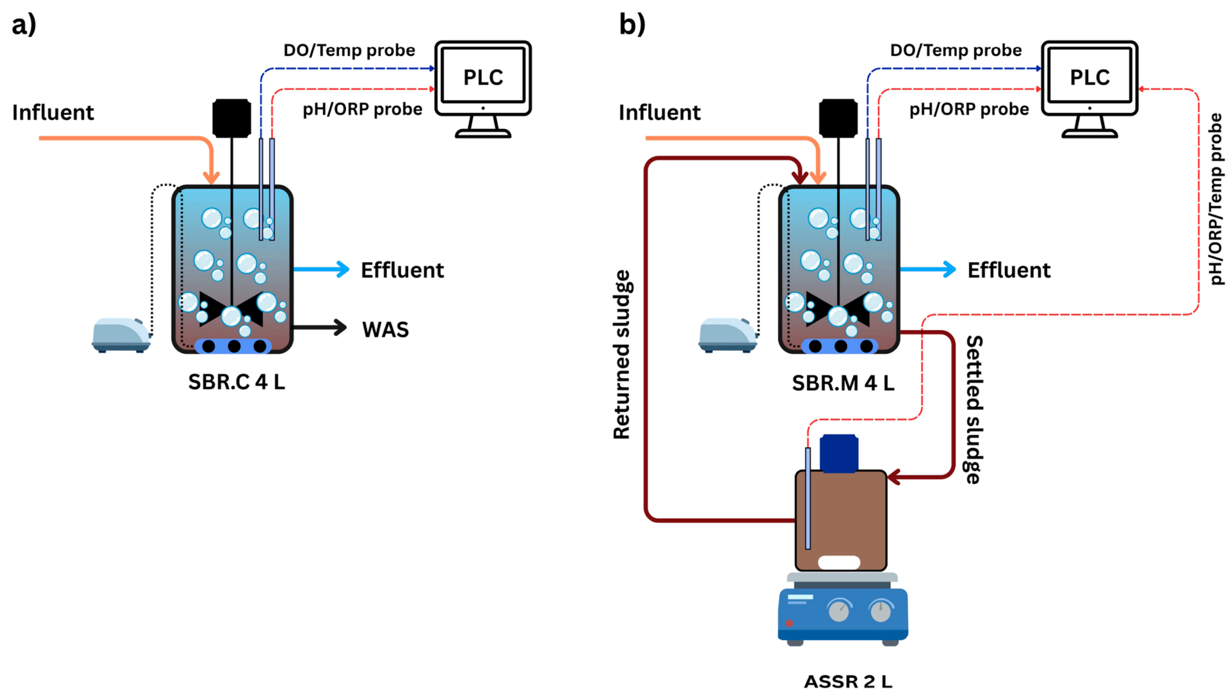

Fig. 1. Process flow diagram of (a) the control reactor (SBR.C) and (b) the integrated main reactor (SBR.M)-ASSR system.

(ORP) in ASSR fluctuated from −400 to −450 mV. The pH was not actively controlled, but the measured pH ranged 7.5–8 in the SBR and 6.7–7 in the ASSR during the experimental period. Mixers were installed in all reactors, and a diffuser was placed in the SBR to maintain a dissolved oxygen (DO) concentration of 2–3 mg/L during the aerobic phase. All reactors were equipped with peristaltic pumps (Watson-Marlow 120 U/DV-220Du-323, USA), pH/ORP probes, and DO probes (Endress+Hauser, The Netherlands), and were automatically controlled via a programmable logic controller (PLC) (Labview, National Instruments, USA) at 0, 2–3, and 0 mg DO/L in the anaerobic, aerobic, and anoxic phases, respectively, in both SBRs. Both reactor systems were placed in a temperature-controlled room (20–22°C).

2.3. Batch experiments: PAO activity

To understand the impact of the alternating anaerobic-aerobic conditions on biological phosphorus removal, a batch test was conducted to assess PAO activity by measuring PO_4^{3-}–P release under anaerobic conditions and uptake under aerobic conditions. At the end of the aerobic phase, mixed liquor was collected from both the SBR and ASSR. Two hundred milliliters of sludge (per reactor) was transferred into 250 mL Schott bottles (Duran, Germany). The anaerobic stage started with 5 min of N_2 purging and was followed by the addition of sodium acetate trihydrate (Merck, Germany) to provide 250 mg COD/L from acetate (equivalent to 234 mg acetate/L). The sludge was incubated anaerobically for 1 h, with samples collected every 15 min to measure PO_4^{3-}–P concentrations. Subsequently, the aerobic phase was initiated by aeration for 1 h without further substrate addition, with sampling every 15 min. All tests were conducted at room temperature (20–22°C). PO_4^{3-}–P concentrations were measured using a UV–Vis spectrophotometer (Hach Lange DR3900, Germany) with LCK 349 test kits (Hach Lange, Germany).

2.4. Analytical methods

2.4.1. Observed sludge yield calculation

The observed sludge yield (Y_{obs}) and sludge reduction efficiency were calculated as the ratio of cumulative generated sludge to cumulative consumed substrate based on Eq. (1) (Chon et al., 2011).

$$Y_{obs} = \frac{\Delta X_{SBR} V_{SBR} + \Delta X_{ASSR} V_{ASSR} + \sum (X_{SBR} Q_{SBR.waste} + X_{ASSR} Q_{ASSR.waste} + X_{eff} Q_{eff}) \times \Delta t}{\sum (S_{in} Q_{in} - S_{eff} Q_{Eff}) \times \Delta t} \quad (1)$$

In this equation, ΔX_{SBR}, ΔX_{ASSR}, and Δt are the change in sludge (g VSS/L) in SBR and ASSR, and time (d), respectively. V_{SBR} and V_{ASSR} are the volumes of SBR and ASSR (L), respectively. $Q_{SBR\ waste}$, Q_{in}, and Q_{eff} are the flow rates of waste sludge from SBR, influent, and effluent (L/d), respectively. $Q_{ASSR\ waste}$ is the flow rate of sludge from ASSR generated during sampling for analysis. S_{in} and S_{eff} are the substrate concentrations of influent and effluent (g tCOD/L), respectively.

2.4.2. Parameters

Several parameters were measured in the influent and effluent of the SBR and in the inlet and outlet of the ASSR. The concentrations of total COD (tCOD), soluble COD (sCOD), NH_4^+-N, NO_2^--N, NO_3^--N, and TP/PO_4^{3-}–P were measured using spectrophotometry-based test kits (LCK 114, LCK 314, LCK 303, LCK 341, LCK 339, LCK 348, Hach Lange LCK, Germany). Mixed liquor suspended solids (MLSS), volatile suspended solids (MLVSS), and sludge volume index (SVI) were analyzed according to standard methods (APHA, 2012). DO, temperature, pH, and ORP were monitored using a portable meter (Endress+Hauser, The Netherlands). Volatile fatty acids (VFAs) were measured using a gas chromatograph equipped with a flame ionization detector (Agilent 7890 A, USA). Soluble EPS (S-EPS), loosely bound EPS (LB-EPS), and tightly bound EPS

(TB-EPS) were extracted using the two-step method (Guo et al., 2020a). The EPS concentration was calculated based on the carbohydrate and protein concentrations. Carbohydrate content was measured via the sulfuric acid method (Dubois et al., 1951) and protein content via a modified Lowry method (Frølund et al., 1995). The particle size distribution (PSD) of sludge samples was determined using a Bluewave laser diffraction particle size analyzer (Microtrac Inc., USA).

2.4.3. Microbial community analysis

Sludge samples from SBR.C, SBR.M, and ASSR were collected in triplicate at the end of the experimental period, after the SBR aerobic phase. The analysed samples included SBR.C (C1–C3), SBR.M (M1–M3), and ASSR (A1–A3). DNA was extracted using the FastDNA® SPIN Kit for Soil (MP Biomedicals, USA) following the manufacturer's instructions. DNA quality and quantity were checked using a Qubit 3.0 fluorometer and the Qubit® dsDNA HS Assay Kit (Life Technologies, USA). The V3–V4 region of the bacterial 16S rRNA gene was amplified using primers 341 F (5′-CCTAYGGGRBGCASCAG-3′) and 806 R (5′-GGACTACNNGGGTATCTAAT-3′), and purified amplicons were sequenced by Novogene Co., Ltd. (Beijing, China) on an Illumina platform using 2 × 250 bp paired-end sequencing. Sequence processing was performed in QIIME2. After quality filtering, trimming, denoising, merging of paired-end reads, and chimera removal, amplicon sequence variants (ASVs) were inferred using DADA2. Taxonomic assignment was performed against the SILVA 138.1 database using the QIIME2 classify-sklearn classifier. Alpha- and beta-diversity analyses were used to characterize microbial community diversity and composition among SBR.C, SBR.M, and ASSR. Predicted functional profiles were generated from the 16S rRNA gene data using PICRUSt2. Predicted gene families were assigned to Kyoto Encyclopedia of Genes and Genomes (KEGG) orthologs and summarized into metabolic pathway categories.

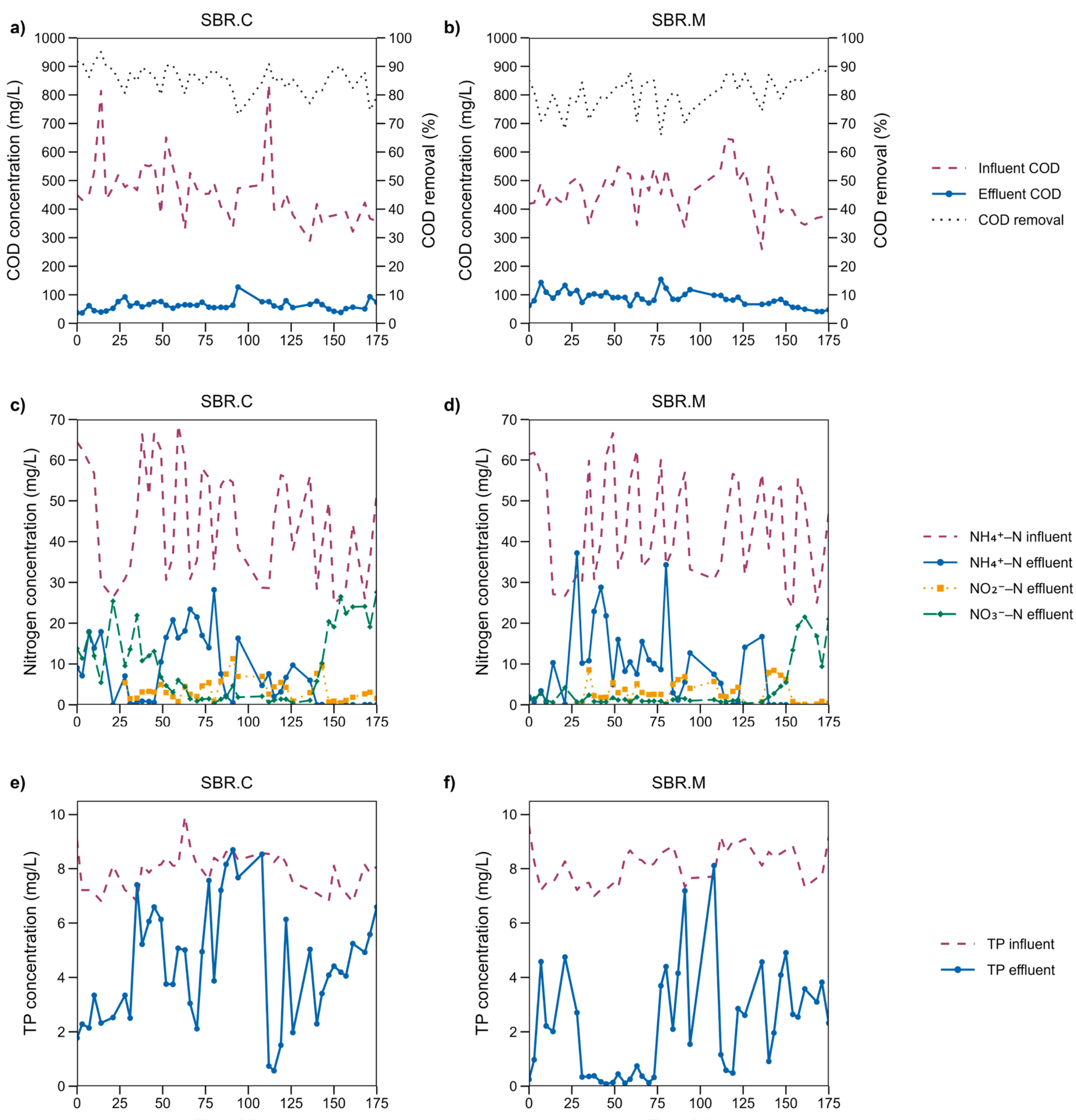

Fig. 2. Pollutant removal performance of SBR.C and SBR.M. (a, b) influent and effluent COD concentration and COD removal; (c, d) NH_4^+-N, NO_2^--N, and NO_3^--N concentrations; (e, f) influent and effluent TP concentrations.

3. Results

3.1. Reactor performance for pollutant removal

Both SBR.C and SBR.M maintained high and relatively stable tCOD removal throughout the operational period (Figs. 2a and 2b). The influent tCOD concentration averaged 450 ± 64 mg/L, while the effluent concentrations in both reactors were generally below 100 mg/L, corresponding to removal efficiencies of approximately 85–90%. SBR.M showed slightly greater temporal variation in effluent than SBR.C, but no persistent deterioration in organic matter removal was observed. The influent and effluent concentrations of NH_4^+-N, NO_2^--N, and NO_3^--N are shown in Figs. 2c and 2d. The influent NH_4^+-N concentrations were comparable between SBR.C and SBR.M, averaging 45 ± 14 and 44 ± 13 mg/L, respectively. The corresponding average NH_4^+-N removal efficiencies were also comparable, at approximately 83 ± 41% in SBR.C and 82 ± 26% in SBR.M. However, the average effluent NO_3^--N concentration was lower in SBR.M than in SBR.C, at 3.6 ± 5.8 and 9.6 ± 8.8 mg/L, respectively. Representative cycle profiles during early operation showed anaerobic sCOD consumption and phosphate release followed by aerobic phosphate uptake in both reactors (Figure S1). SBR.C showed greater ammonium oxidation and nitrate accumulation, whereas SBR.M exhibited anaerobic ammonium release and transient nitrite accumulation, followed by decreasing NO_2^--N and NO_3^--N concentrations during the anoxic phase.

TP removal differed markedly between the two systems (Figs. 2e and 2f). Removal efficiencies ranged from 23% to 90% in SBR.C, with an average of 48 ± 24%, and from 41% to 98% in SBR.M, with an average of 75 ± 24%. The highest TP removal in SBR.M was observed during approximately the first 80 d of operation, after which the performance became less pronounced. The PAO activity tests further demonstrated differences among the sludge samples (Figure S2). In SBR.C sludge, PO_4^{3-}–P increased from 4.1 to 13.3 mg/L during the anaerobic phase, but no substantial phosphate uptake was observed during the subsequent aerobic phase. In SBR.M sludge, anaerobic phosphate release reached approximately 13.2 mg/L and was followed by aerobic phosphate uptake at a rate of 1.93 mg/L/h. ASSR sludge also released phosphate during anaerobic incubation, with the concentration increasing from 98.2 to 113.4 mg/L. After exposure to aerobic conditions, the concentration decreased to approximately 80 mg/L within 2 h.

3.2. Observed sludge yield and transformations in the ASSR

The integration of the ASSR into the sludge return line substantially reduced sludge production in SBR.M compared with SBR.C (Fig. 3). Based on Fig. 3a, the slope-derived observed sludge yield was 0.288 g VSS/g COD for SBR.C and 0.166 g VSS/g COD for SBR.M, corresponding to an observed sludge yield reduction of approximately 42%. During most of the operational period, based on Fig. 3b, SBR.M consistently showed lower values than SBR.C.

The concentrations of COD, ammonium, and phosphate in the ASSR, presented in Fig. 4, also indicated substantial transformation of the sludge during anaerobic retention. Total COD decreased from 16 ± 2.7 g/L at the ASSR inlet to 14 ± 2.9 g/L at the outlet. In contrast, sCOD increased from 47 ± 12 to 208 ± 60 mg/L, and the NH_4^+-N concentration also increased from 12 ± 9 to 66 ± 20 mg/L across the ASSR. In addition, the PO_4^{3-}–P concentration at the ASSR inlet averaged 11.3 ± 2.8 mg/L, whereas the outlet concentration ranged from approximately 80 to 250 mg/L. After approximately day 70, phosphate release gradually declined, although the concentration remained elevated at approximately 125 mg/L at the end of the experiment. Volatile fatty acids (VFAs) were also detected in the ASSR, primarily as acetate and propionate. The total VFA concentration reached a maximum of 98 ± 1.5 mg/L on day 28 but subsequently declined after approximately day 75 and remained low during the later operational period. The declines in VFA concentration and phosphate accumulation occurred over a similar operational period.

Based on Fig. 3a, the sludge production rates were 1.02 ± 0.16 g VSS/d in SBR.C and 0.51 ± 0.22 g VSS/d in SBR.M, corresponding to a system-level difference of 0.51 g VSS/d. To evaluate how much of this difference was represented by solids transformation within the ASSR, a simplified flow-based VSS balance was applied. The average VSS concentrations of the sludge entering and leaving the ASSR were 9.56 and 8.92 g/L, respectively. At the constant sludge-interchange rate of 200 mL/d, this inlet–outlet difference corresponded to an estimated net VSS decrease of approximately 0.13 g VSS/d. Thus, the net VSS decrease across the ASSR was equivalent to approximately 25% of the difference in sludge production between the two systems.

3.3. Sludge characteristics and settleability

3.3.1. MLSS, MLVSS, and sludge loading

The solids concentrations showed different temporal patterns among the three reactors (Figure S3). In SBR.C, MLSS and MLVSS remained

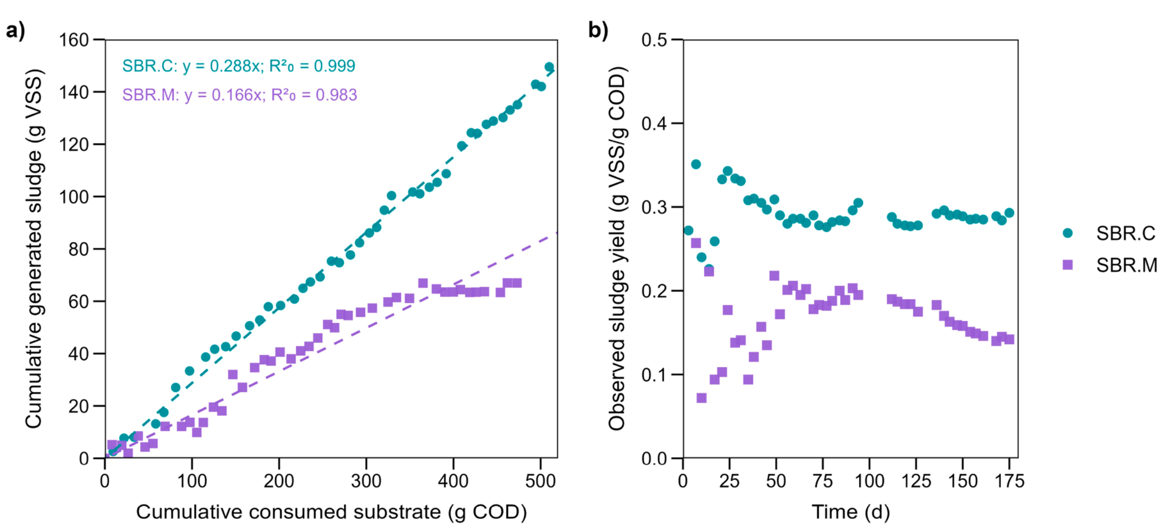

Fig. 3. Comparison of sludge production and observed sludge yield in SBR.C and SBR.M. (a) Cumulative sludge production versus cumulative consumed substrate and (b) observed sludge yield over time.

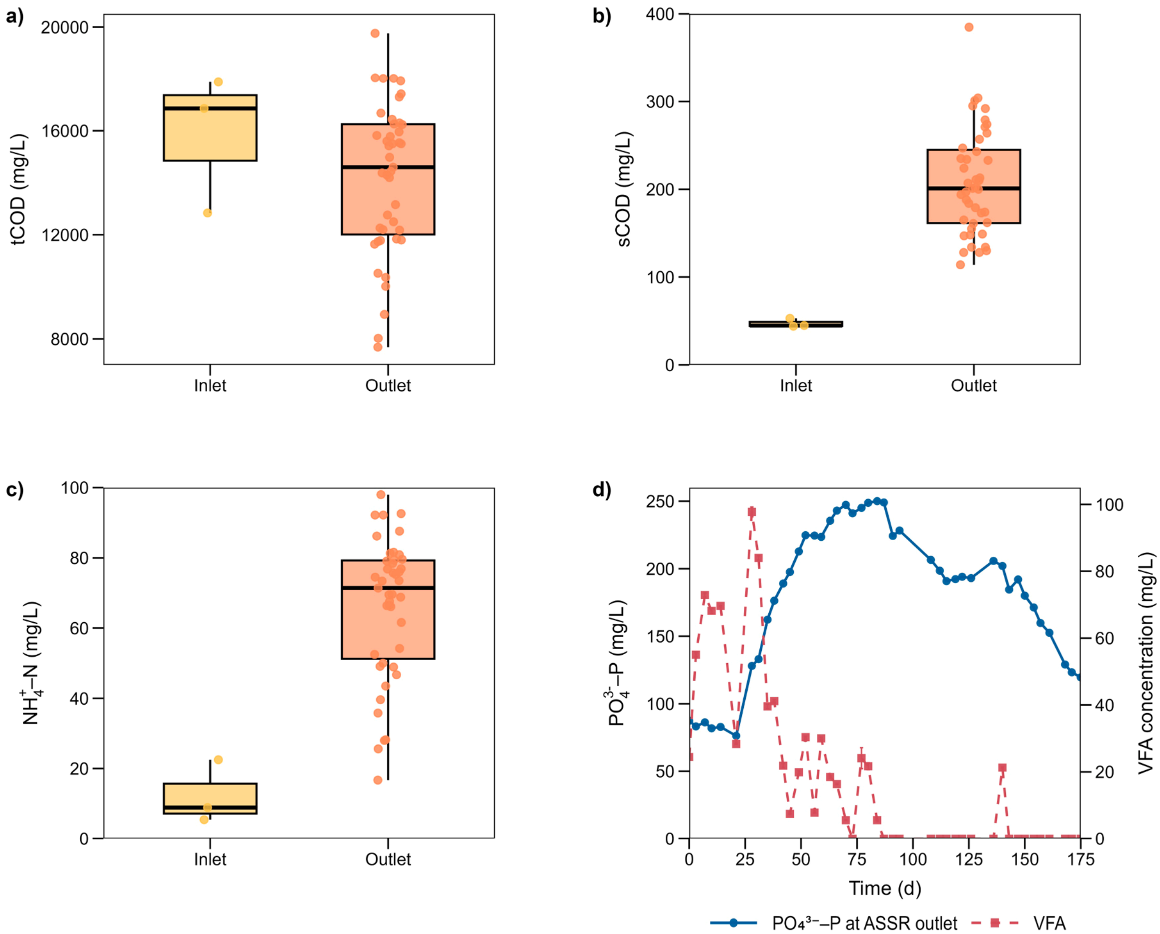

Fig. 4. Sludge transformation in the inlet and outlet of the ASSR. (a) tCOD, (b) sCOD, (c) NH_4^+-N, (d) PO_4^{3-}–P and VFA concentrations during operational.

relatively stable at approximately 5–7 and 3.5–5 g/L, respectively, with an MLVSS/MLSS ratio of 0.75–0.80 (Figure S3a). In SBR.M, both MLSS and MLVSS gradually decreased during operation, accompanied by a slight decrease in the MLVSS/MLSS ratio (Figure S3b). The largest decrease was observed in the ASSR, where MLSS declined from approximately 16 to 6 g/L and MLVSS from approximately 10 to 4 g/L (Figure S3c). Although the volumetric sludge interchange was maintained at 200 mL/d, the solids loading rate to the ASSR decreased from approximately 1.2–1.3 kg TSS/m^3/d during the initial operational period (0–80 d) to 0.6–0.8 kg TSS/m^3/d during the later period (80–175 d). This decline coincided with the increase in SVI in SBR.M.

3.3.2. EPS composition, settleability, and particle-size distribution

The sludge settleability differed between the two SBRs (Fig. 5a). The SVI of SBR.C ranged between 45 and 173 mL/g, whereas SBR.M reached values in the range of 93–221 mL/g during the operational period. Despite the higher SVI in SBR.M, effluent suspended-solids concentrations remained comparable between the two systems, generally ranging from 60 to 120 mg/L. The total EPS concentration was lowest in the ASSR at 25.35 ± 0.17 mg/g VSS, compared with 38.72 ± 0.11 mg/g VSS in SBR.C and 45.86 ± 0.18 mg/g VSS in SBR.M (Fig. 5b). In contrast, the soluble EPS fraction increased from 3.35 ± 0.01 mg/g VSS in SBR.C to 3.51 ± 0.04 mg/g VSS in SBR.M and 3.67 ± 0.11 mg/g VSS in the ASSR. The differences in soluble EPS among the reactors were statistically significant ($p < 0.05$). The particle size distributions also differed among the reactors (Fig. 5c). The dominant particle-size peak was approximately 176 μm in SBR.C, compared with 48 μm in SBR.M and 40 μm in the ASSR.

3.3.3. Microbial community and predicted functional profiles

Fig. 6 presents the relative abundance of microbial communities at the family level, while Figure S4 presents microbial communities at the phylum and genus levels. The results showed that the dominant families in SBR.C included Chitinophagaceae (9.3%), Saprospiraceae (7.5%), Rhodocyclaceae (7.1%), Moraxellaceae (6.5%), and Comamonadaceae (5.8%). At the phylum level, it was dominated by Proteobacteria (41.8%) and Bacteroidota (28%), followed by Myxococcota (7.3%) and Gemmatimonadota (4.4%). Predatory Bdellovibrionota represented 0.32% of the community. In contrast, SBR.M showed a different microbial community profile from SBR.C. At the family level, Gemmatimonadaceae increased from 4.4% in SBR.C to 9.4% in SBR.M, while Saprospiraceae increased from 7.5% to 10.8%. In contrast, Chitinophagaceae decreased from 9.3% to 1.2%. At the phylum level, compared to SBR.C, Proteobacteria decreased to 35.8%, whereas Gemmatimonadota increased to 9.4%, Bdellovibrionota to 3.2%, and Patescibacteria to 4.7%. Meanwhile, the ASSR community was dominated by Bacteroidota (41.1%), followed by Proteobacteria (24.4%), Patescibacteria (5.5%), and Bdellovibrionota (2.1%). The most abundant families included Saprospiraceae (13.4%), Gemmatimonadaceae (6.9%), Comamonadaceae (6.8%), and Bacteroidetes_vadinHA17 (5.4%). At the genus level, Lentimicrobium (2.8%), Haliangium (2.9%), and Bdellovibrio (1.6%) were detected in the ASSR.

Several genera commonly associated with nitrogen and phosphorus transformations differed between SBR.C and SBR.M. Denitratisoma increased from 0.8% in SBR.C to 1.8% in SBR.M, while Pseudomonas increased from 0.3% to 0.9%. Thauera decreased from 2% to 1.2%. Nitrosomonas represented 0.6% of the SBR.M community, while *Candidatus* Nitrotoga increased from 0.2% in SBR.C to 3.2% in SBR.M.

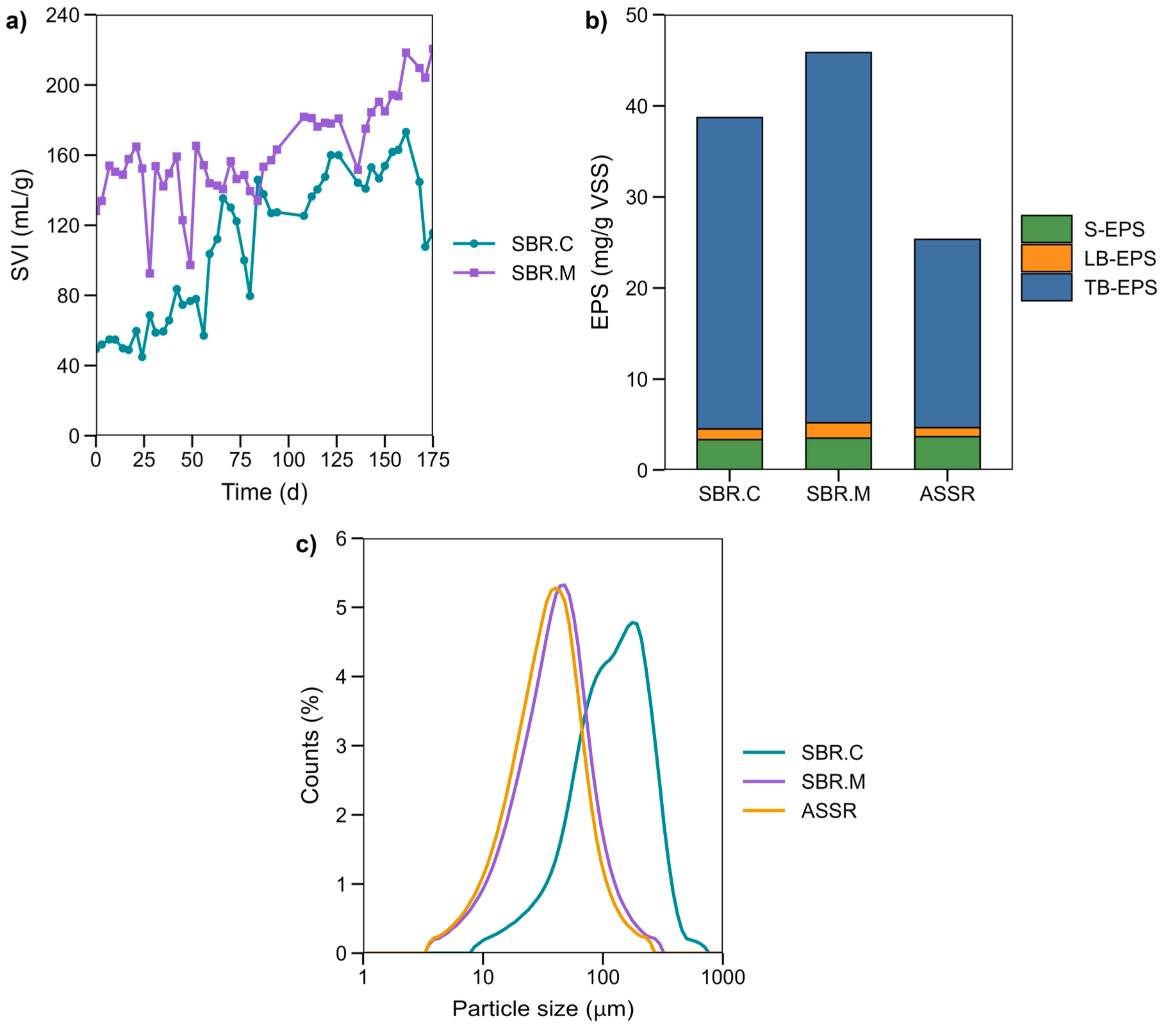

Fig. 5. Sludge characteristics and settleability. (a) sludge volume index, (b) extracellular polymeric substance fractions, and (c) particle size distribution.

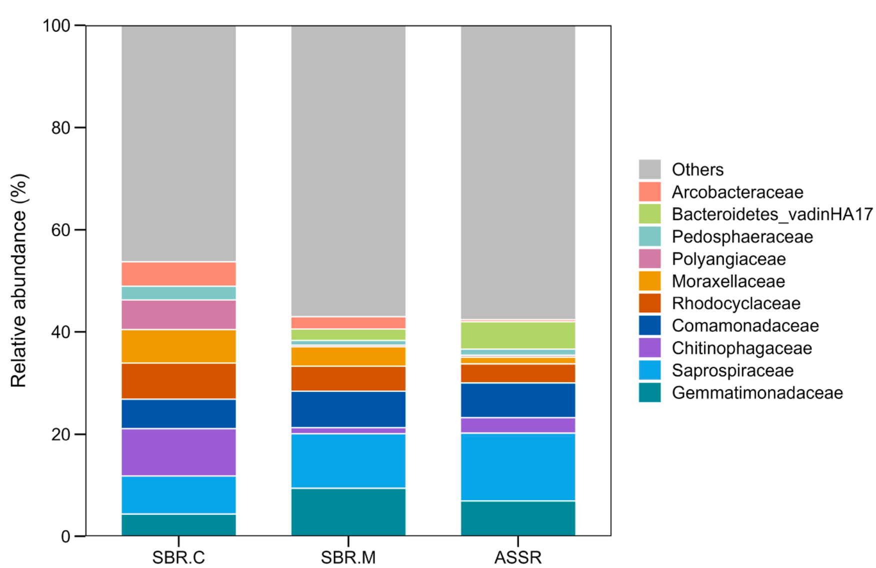

Fig. 6. Family-level relative abundance of microbial communities in SBR.C, SBR.M, and the ASSR.

Potential PAO-associated genera detected in SBR.M included Dechloromonas, which increased from 0.05% to 0.9%, and Gemmatimonas, which increased from 0.3% to 0.7%.

The predicted functional profiles derived from the 16S rRNA gene data also differed among the reactors (Figures S5 and S6). SBR.C showed a relatively greater predicted representation of biosynthetic and cellular-maintenance functions, whereas SBR.M and the ASSR showed a relatively greater predicted representation of pathways related to organic matter degradation and energy conversion. These results represent inferred functional potential based on taxonomic composition rather than direct measurements of gene expression or metabolic activity.

4. Discussion

4.1. Organic and nutrient removal performance

The comparable tCOD removal in SBR.C and SBR.M indicates that the integration of the ASSR did not substantially impair the overall organic matter removal capacity of the SBR under the tested conditions. The slightly greater variability in the SBR.M effluent may have resulted from the return of soluble microbial products, soluble humic substances, and partially hydrolyzed EPS generated during anaerobic sludge transformation in the ASSR (Corsino et al., 2023). However, the absence of persistent COD accumulation in the effluent suggests that a substantial fraction of these returned compounds was subsequently degraded in the SBR. Similar studies by Peng et al. (2023) have shown that the inclusion of ASSR units in the sludge return line does not necessarily compromise COD removal.

The comparable average NH_4^+-N removal efficiencies in SBR.C and SBR.M indicate that repeated sludge exposure to the anaerobic ASSR conditions did not substantially affect overall NH_4^+-N removal in the integrated system, consistent with observations reported for other SBR–ASSR configurations (Huang et al., 2021). Despite the additional NH_4^+-N load generated through sludge mineralization in the ASSR, the average effluent NH_4^+-N concentration of SBR.M remained comparable to that of SBR.C. The lower effluent NO_3^--N concentration in SBR.M indicated less nitrate accumulation, but did not reveal whether this resulted from higher nitrate reduction or lower nitrate production. The COD mass balance showed that the sludge return from the ASSR added an additional COD load equivalent to up to 47% of the influent COD load to the SBR.M. The return flow may have contained soluble organic compounds released through sludge hydrolysis and intracellular storage compounds that could be used for denitrification in SBR.M (Morello et al., 2024b; Zhou et al., 2015). However, the biodegradable fraction of this COD or the proportion specifically used for denitrification was not determined. Therefore, ASSR-derived carbon is considered a plausible contributor to the lower nitrate accumulation in SBR.M. Because TN, organic nitrogen, gaseous nitrogen products, and pathway-specific conversion rates were not measured, the relative contributions of nitrification, denitrification, mineralization, and biomass assimilation could not be resolved.

This accumulation of NO_3^--N in SBR.C at the beginning of the anaerobic phase may result in lower TP removal compared to SBR.M. Wang et al. (2015) reported that residual nitrate allows denitrifying heterotrophs to compete with PAOs for readily biodegradable carbon, thereby reducing the amount available for anaerobic storage and subsequent aerobic phosphate uptake. With approximately 34 mg acetate/L in the influent and around 10 mg/L of NO_3^--N remaining at the start of the anaerobic phase, nitrate reduction could have consumed a substantial fraction of the available acetate. The PAO activity test was consistent with weak EBPR performance in SBR.C, where anaerobic phosphate release occurred, but it was not followed by substantial aerobic uptake. Because acetate was available throughout the batch test, the limited uptake was unlikely to result solely from short-term carbon limitation. Recurrent nitrate exposure and the long-term limited availability of carbon for PAO storage metabolism may also have reduced the capacity for phosphate uptake (Zhang et al., 2024).

SBR.M achieved higher TP removal than SBR.C, particularly during the first 80 d of operation. The additional anaerobic exposure in the ASSR may have improved carbon availability for phosphorus cycling through sludge hydrolysis, fermentation, and subsequent cell internal carbon storage before the biomass was returned to SBR.M (Ferrentino et al., 2021; Zhao et al., 2021). PAO activity tests confirmed that the SBR.M-ASSR circulated biomass retained phosphorus storage capacity. Unlike SBR.C sludge, sludge in SBR.M showed anaerobic phosphate release followed by measurable aerobic uptake, while batch tests indicated phosphate uptake by ASSR sludge after transfer to aerobic conditions.

However, the higher TP removal was not sustained over the operational period. Its decline after day 80 coincided with lower ASSR solids loading, VFA production, and phosphate release in the ASSR. The relationship between deteriorating settleability, reduced ASSR solids loading, and phosphorus performance is discussed further in Section 4.3. Nevertheless, SBR.M maintained better TP removal than SBR.C after the decline in VFA production, indicating that soluble VFAs were not the only factor controlling phosphorus removal. Intracellularly stored carbon and repeated circulation of PAO-capable biomass may also have contributed (Sun et al., 2021). Overall, the enhanced phosphorus removal was a transient operational response rather than a stable long-term outcome.

4.2. Interpretation of observed sludge yield reduction and associated mechanisms

The observed sludge yield was 42% lower in SBR.M than in SBR.C. This difference likely resulted from two co-occurring features of the tested configuration: the longer effective SRT of the SBR.M-ASSR combination and the repeated anaerobic–aerobic exposure of sludge circulated through the ASSR (Cheng et al., 2021). Longer biomass retention can reduce observed yield by increasing endogenous respiration, maintenance requirements, decay, and biomass turnover, while repeated redox transitions may alter the utilization and redistribution of organic carbon (Semblante et al., 2016b). Because the effective SRTs in the two systems were different, the respective contributions of biomass retention and ASSR exposure could not be quantified separately. Therefore, the lower observed yield should be interpreted as the net effect of the tested SBR–ASSR configuration rather than being attributed solely to direct solids destruction in the ASSR. These findings are consistent with previous studies demonstrating that ASSR integration can reduce observed sludge yield by 30–50% (Huang et al., 2019).

Anaerobic conditions in the ASSR promoted sludge degradation, as indicated by increased sCOD, NH_4^+-N, VFA, and PO_4^{3-}-P concentrations, reflecting hydrolysis, fermentation, organic nitrogen mineralization, and the release of intracellularly stored phosphorus as phosphate (Foladori et al., 2015; Wang et al., 2020). However, tCOD decreased by only approximately 11%, indicating that organic matter was mainly redistributed from particulate biomass into soluble and mineralized fractions rather than extensively removed from the system (Jing et al., 2026). Consequently, the average net VSS decrease measured across the ASSR was only approximately 0.13 g VSS/d, equivalent to about 25% of the difference in sludge production between SBR.C and SBR.M. The remaining unaccounted 75% indicates that most of the reduction occurred through lower net biomass formation and greater biomass turnover throughout the integrated SBR.M-ASSR system. Organic compounds released in the ASSR remained within the system and, after being returned to SBR.M, may have been used for maintenance and energy generation, further mineralized, stored intracellularly, or recycled through lysis–cryptic-growth processes, with only part converted into new biomass (Corsino et al., 2023). To be able to fully understand the fate of the carbon fraction in this system, more detailed analysis should be performed, e.g., by labeled substrate tracking. However, these proposed system-level processes provide a plausible explanation for the remaining reduction in observed sludge yield.

The microbial communities differed among SBR.C, SBR.M, and the ASSR. These differences cannot be attributed exclusively to reactor operation because the inocula had different prior conditioning histories. Although both originated from the same WWTP, the ASSR inoculum had previously been conditioned under anaerobic thermophilic conditions, which may have favored hydrolytic and fermentative populations during start-up (Monteiro et al., 2026). Nevertheless, approximately 90 d of acclimation, equivalent to about nine nominal ASSR retention times, together with continuous sludge exchange between SBR.M and the ASSR, likely imposed sustained selection under the respective reactor conditions. The observed communities therefore reflect both initial inoculum conditioning and subsequent long-term reactor selection, whose relative contributions could not be separated.

Within this interpretative scope, the greater relative abundance of Bacteroidota, Saprospiraceae, Bdellovibrionota, and other groups associated with polymer degradation in SBR.M and the ASSR was consistent with an environment favoring the transformation and reuse of biomass-derived organic matter (Cong et al., 2025; Semblante et al., 2017; Xu et al., 2018). Predicted functional profiles likewise indicated a greater representation of pathways related to organic-matter degradation and energy conversion in the integrated system. However, these predictions reflect inferred functional potential rather than measured metabolic activity and therefore provide supporting, but not conclusive, evidence for the proposed mechanisms underlying the lower observed sludge yield.

4.3. Sludge characteristics, floc deterioration, and operational trade-offs

The lower observed sludge yield in the integrated system was accompanied by poorer sludge settleability, with SVI values in SBR.M exceeding 200 mL/g. Nevertheless, effluent suspended-solids concentrations remained comparable between SBR.C and SBR.M, COD removal was maintained, and effluent solids were included in the observed-yield calculation. Therefore, the lower yield cannot be attributed to unaccounted biomass washout. Corsino et al. (2023) similarly reported that poorer settleability in an ASSR system operated at long SRT, possibly associated with filamentous bacteria. Quiescent settling and controlled decanting were sufficient to retain sludge under the tested laboratory conditions. However, the reduced sludge compaction could require longer settling periods, lower decant rates, or greater separation capacity at larger scale, making settleability deterioration an important scale-up constraint.

The changes in EPS composition and PSD provide a consistent explanation for this poorer settling behavior. The sludge from the ASSR contained the lowest total EPS concentration and the highest soluble EPS fraction, suggesting that part of the floc-associated matrix was solubilized during anaerobic retention, weakening floc cohesion (Corsino et al., 2020; Guo et al., 2020a). This was further supported by smaller particle sizes in SBR.M and ASSR (48 µm and 40 µm, respectively), compared to a dominant particle size of approximately 176 µm in SBR.C. The higher total EPS concentration in SBR.M may reflect the accumulation of less degradable EPS fractions due to sludge cycling or additional EPS production in response to repeated redox transitions (Guo et al., 2020a; Zhao et al., 2023).

The deterioration in sludge settleability also affected ASSR operation. At a constant sludge-interchange rate, the lower concentration of settled sludge withdrawn from SBR.M reduced the ASSR solids loading from approximately 1.2–1.3 to 0.6–0.8 kg TSS/m^3/d, thereby decreasing the particulate organic matter and poly-P-containing biomass available for hydrolysis, fermentation, and phosphate release. This observation provides a plausible process-level link to the concurrent decline in VFA production, phosphate release, and TP removal during the later operational period. Smaller flocs may also have altered internal oxygen and substrate gradients (Zou et al., 2025), although their effects on PAO and denitrifier activity could not be established from the available data. Overall, sludge reduction was achieved without deterioration in effluent suspended solids or COD removal under the tested conditions, but poorer sludge compaction and reduced ASSR loading lowered operational robustness and represent a significant engineering trade-off for scale-up.

4.4. Implications and scale-up considerations

From an engineering perspective, the main implication of this study is that the ASSR should be considered as an integrated sludge management unit rather than as an independent sludge destruction reactor. Its performance should be evaluated at the plant level, based on the net amount of sludge requiring further treatment and disposal while maintaining the required effluent quality. The design objective is not necessarily to maximize solids loss within the ASSR itself, but to achieve lower overall sludge production without compromising the operation of the main biological reactor.

Scale-up requires ASSR volume, sludge exposure to the anaerobic famine conditions, and settleability to be optimized together. In this study, the 2 L ASSR resulted from the design value of 10% biomass exchange, volumetric loading rate of 1 kg/m^3/d to the ASSR, MLSS concentration in the SBR.M of 5 g/L and a target side-stream retention time of 10 d. The resulting fixed volumetric exchange ratio of 200 mL/d and ASSR-to-SBR volume ratio of 0.5 was a practical experimental configuration rather than a recommended full-scale ratio. Because the sludge concentration varied during operation, the fixed volumetric exchange resulted in a variable loading rate to the ASSR, ranging from 0.6 to 1.3 kg TSS/m^3/d. Full-scale design should therefore be based on the sludge mass in the activated sludge tanks, the sludge mass exchange ratio, and the duration and frequency of anaerobic exposure, rather than on reactor volume or volumetric interchange alone. Sludge pre-concentration, a smaller ASSR, and shorter retention times could reduce the required footprint, but their effects on sludge reduction and settleability must be evaluated simultaneously. Previous ASSR studies indicate that settleability responses depend on the selected retention time and interchange conditions and may deteriorate during long-term operation (Semblante et al., 2016a; Velho et al., 2016; Ye et al., 2008). This means that volumetric exchange will lead to fluctuations in ASSR loading rates, similar to the observations in our study. Accordingly, sludge transfer should be controlled on a solids-mass basis and depending on the sludge concentrations in the return sludge line after final clarification.

A relatively large ASSR would increase the required footprint and capital investment, but its economic implication should not be assessed from reactor volume alone. The appropriate comparison is between the annualized capital expenditure (CAPEX) and operating expenditure (OPEX) of the ASSR and the avoided costs of sludge thickening, dewatering, further treatment, transport, and disposal. Thus, increasing the total biological treatment volume up to 150% would not necessarily result in a proportional increase in total plant cost, because part of the additional expenditure may be offset by lower downstream sludge-management requirements. The economic feasibility of ASSR integration will depend on whether these avoided costs exceed the annualized cost of the additional side-stream unit. Therefore, a plant-wide techno-economic assessment is required to determine this balance and to identify the combination of ASSR volume, solids loading, and retention time that provides the lowest overall treatment cost.

5. Conclusions

The main conclusions of this study are:

- Integrating the ASSR with the SBR reduced the observed sludge yield by 42%, while maintaining comparable COD and ammonium removal. Comparable effluent suspended solids, included in the solids balance, confirmed that the lower yield was not caused by sludge washout.
- The net VSS decrease across the ASSR explained only part of the lower observed sludge yield, while the remaining difference likely resulted from lower net biomass formation and greater biomass turnover under the longer effective SRT and repeated anaerobic–aerobic exposure of the integrated system.

- ASSR operation initially increased VFA production and phosphate release, which coincided with higher phosphorus removal. These benefits weakened as the solids loading to the ASSR decreased. At the same time, sludge reduction was accompanied by smaller flocs and SVI values above 200 mL/g. Although this did not increase effluent suspended solids concentrations under the tested conditions, poorer settleability reduced operational robustness and represented the main engineering trade-off.
- The ASSR-to-SBR volume ratio of 0.5 resulted from the selected 10 d side-stream retention time and is not a full-scale design recommendation. Future work should define the operating window for solids loading, retention time, and sludge interchange that maintains sludge reduction with acceptable settleability and a smaller ASSR volume, in order to establish design parameters for full-scale application.

CRediT authorship contribution statement

Merle de Kreuk: Writing – review & editing, Validation, Supervision, Methodology, Funding acquisition, Formal analysis, Conceptualization. **Ralph E.F. Lindeboom:** Writing – review & editing, Validation, Supervision, Methodology, Formal analysis, Conceptualization. **Alexander Hendriks:** Writing – review & editing, Validation, Supervision, Methodology, Formal analysis, Conceptualization. **Lenno van den Berg:** Writing – review & editing, Validation, Supervision, Methodology, Formal analysis, Conceptualization. **Muhammad Fauzul Imron:** Writing – original draft, Visualization, Validation, Supervision, Methodology, Investigation, Funding acquisition, Formal analysis, Data curation, Conceptualization.

Declaration of Generative AI and AI-assisted technologies in the writing process

During the preparation of this work, the author(s) used ChatGPT and Grammarly in order to refine the language. After using this tool/service, the author(s) reviewed and edited the content as needed and take(s) full responsibility for the content of the publication.

Declaration of Competing Interest

The authors declare that they have no known competing financial interests or personal relationships that could have appeared to influence the work reported in this paper.

Acknowledgements

The authors would like to thank the Ministry of Finance of the Republic of Indonesia and the Indonesia Endowment Fund for Education (LPDP) for funding the first author's PhD program. The authors would also like to thank the Waterkracht collective, including the Waterschap Zuiderzeeland, Waterschap the Vallei & Veluwe, Waterschap the Rijn en IJssel, Waterschap the Vechtstromen, and Waterschap Drents Overijsselse Delta, as well as Haskoning in the Netherlands, for supporting this research.

Appendix A. Supporting information

Supplementary data associated with this article can be found in the online version at doi:10.1016/j.psep.2026.109520.

References

APHA, 2012. Standard Methods for Examination of Water and Wastewater. Washingt. Am. Public Heal. Assoc.

Cheng, C., Geng, J., Lin, Y., Yu, Q., Wang, Y., Man, F., Ren, H., 2022. A metabolomic view of how the anaerobic side-stream reactors achieves in-situ sludge reduction. J. Clean. Prod. 368, 132990. https://doi.org/10.1016/j.jclepro.2022.132990.

Cheng, C., Geng, J., Zhou, Z., Yu, Q., Gao, R., Shi, Y., Wang, L., Ren, H., 2021. A novel anoxic/aerobic process coupled with micro-aerobic/anaerobic side-stream reactor filled with packing carriers for in-situ sludge reduction. J. Clean. Prod. 311, 127192. https://doi.org/10.1016/j.jclepro.2021.127192.

Chon, D.-H., Rome, M., Kim, Y.M., Park, K.Y., Park, C., 2011. Investigation of the sludge reduction mechanism in the anaerobic side-stream reactor process using several control biological wastewater treatment processes. Water Res. 45, 6021–6029. https://doi.org/10.1016/j.watres.2011.08.051.

Cong, D., Liu, J., Yu, S., Wu, P., Qin, M., 2025. Assessment of anthropogenic impacts on water quality and microbial communities in the Heilongjiang Maolan Gou National Nature Reserve. Microb. Ecol. 88, 134. https://doi.org/10.1007/s00248-025-02645-7.

Corsino, S.F., Carabillò, M., Cosenza, A., De Marines, F., Di Trapani, D., Traina, F., Torregrossa, M., Viviani, G., 2023. Insights on mechanisms of excess sludge minimization in an oxic-settling-anaerobic process under different operating conditions and plant configurations. Chemosphere 312, 137090. https://doi.org/10.1016/j.chemosphere.2022.137090.

Corsino, S.F., de Oliveira, T.S., Di Trapani, D., Torregrossa, M., Viviani, G., 2020. Simultaneous sludge minimization, biological phosphorous removal and membrane fouling mitigation in a novel plant layout for MBR. J. Environ. Manag. 259, 109826. https://doi.org/10.1016/j.jenvman.2019.109826.

Dubois, M., Gilles, K., Hamilton, J.K., Rebers, P.A., Smith, F., 1951. A colorimetric method for the determination of sugars. Nature 168, 167. https://doi.org/10.1038/168167a0.

EurEau, 2021. Waste water treatment - sludge management. Brief. Note Eur. Fed. Natl. Assoc. Water Serv.

Ferrentino, R., Langone, M., Andreottola, G., 2021. Sludge reduction by an anaerobic side-stream reactor process: a full-scale application. Environ. Chall. 2, 100016. https://doi.org/10.1016/j.envc.2020.100016.

Ferrentino, R., Langone, M., Fiori, L., Andreottola, G., 2023. Full-scale sewage sludge reduction technologies: a review with a focus on energy consumption. Water 15, 615. https://doi.org/10.3390/w15040615.

Ferrentino, R., Langone, M., Merzari, F., Tramonte, L., Andreottola, G., 2016. A review of anaerobic side-stream reactor for excess sludge reduction: configurations, mechanisms, and efficiency. Crit. Rev. Environ. Sci. Technol. 46, 382–405. https://doi.org/10.1080/10643389.2015.1096879.

Foladori, P., Velho, V.F., Costa, R.H.R., Bruni, L., Quaranta, A., Andreottola, G., 2015. Concerning the role of cell lysis-cryptic growth in anaerobic side-stream reactors: the single-cell analysis of viable, dead and lysed bacteria. Water Res. 74, 132–142. https://doi.org/10.1016/j.watres.2015.01.042.

Frølund, B., Griebe, T., Nielsen, P.H., 1995. Enzymatic activity in the activated-sludge floc matrix. Appl. Microbiol. Biotechnol. 43, 755–761. https://doi.org/10.1007/BF00164784.

Gao, N., Kamran, K., Quan, C., Williams, P.T., 2020. Thermochemical conversion of sewage sludge: a critical review. Prog. Energy Combust. Sci. 79, 100843. https://doi.org/10.1016/j.pecs.2020.100843.

Gonzalez, A., van Lier, J.B., de Kreuk, M.K., 2021. The role of growth media on composition, bioconversion and susceptibility for mild thermal pre-treatment of waste activated sludge. J. Environ. Manag. 298, 113491. https://doi.org/10.1016/j.jenvman.2021.113491.

Guo, H., Felz, S., Lin, Y., van Lier, J.B., de Kreuk, M., 2020a. Structural extracellular polymeric substances determine the difference in digestibility between waste activated sludge and aerobic granules. Water Res. 181, 115924. https://doi.org/10.1016/j.watres.2020.115924.

Guo, H., van Lier, J.B., de Kreuk, M., 2020b. Digestibility of waste aerobic granular sludge from a full-scale municipal wastewater treatment system. Water Res. 173, 115617. https://doi.org/10.1016/j.watres.2020.115617.

Huang, H., Ekama, G.A., Biswal, B.K., Dai, J., Jiang, F., Chen, G.-H., Wu, D., 2019. A new sulfidogenic oxic-settling anaerobic (SOSA) process: the effects of sulfur-cycle bioaugmentation on the operational performance, sludge properties and microbial communities. Water Res. 162, 30–42. https://doi.org/10.1016/j.watres.2019.06.051.

Huang, H., Ekama, G., Deng, Y.-F., Chen, G.-H., Wu, D., 2021. Identifying the mechanisms of sludge reduction in the sulfidogenic oxic-settling anaerobic (SOSA) process: side-stream sulfidogenesis-intensified sludge decay and mainstream extended aeration. Water Res. 189, 116608. https://doi.org/10.1016/j.watres.2020.116608.

Jing, Xinyu, Wang, D., Qin, L., Meng, H., Song, Y., Jing, Xiaosheng, Zhu, M., Lin, Y., Wu, R., Li, J., 2026. Effect of side-stream conditions on the release of dissolved organic matter in the side-stream enhanced biological phosphorus removal process. Environ. Sci. Water Res. Technol. 12, 2144–2155. https://doi.org/10.1039/D6EW00198J.

Monteiro, J.P., Srinivas, R., van den Berg, L., Mirzaee, P., Cruzeiro, C., Alcina Pereira, M., Vilar, V.J.P., de Kreuk, M.K., Pavez-Jara, J., 2026. Mild thermal pre-treatment of waste activated sludge combined with hydrogen peroxide and iron addition. J. Clean. Prod. 568, 148641. https://doi.org/10.1016/j.jclepro.2026.148641.

Morello, R., Di Capua, F., Farmer, M., Dunlap, P., Qin, C.D., Kozak, J.A., Spasiano, D., Sabba, F., 2024a. Minimizing biological sludge generation in a sidestream enhanced biological phosphorus removal (S2EBPR) system: full-scale evaluation and modeling insights. Environ. Sci. Water Res. Technol. 10, 1666–1675. https://doi.org/10.1039/D4EW00115J.

Morello, R., Di Capua, F., Kalkan Aktan, Ç., Yilmaz, T., Esposito, G., Pirozzi, F., Fratino, U., Spasiano, D., Sahinkaya, E., 2024b. Unravelling the impact of oxic-settling-anaerobic cycle implementation and solid retention time on sludge generation, membrane operation, and contaminant removal in membrane

bioreactors. Chem. Eng. J. 496, 153800. https://doi.org/10.1016/j.cej.2024.153800.
Patel, A., Arkatkar, A., Singh, S., Rabbani, A., Solorza Medina, J.D., Ong, E.S., Habashy, M.M., Jadhav, D.A., Rene, E.R., Mungray, A.A., Mungray, A.K., 2021. Physico-chemical and biological treatment strategies for converting municipal wastewater and its residue to resources. Chemosphere 282, 130881. https://doi.org/10.1016/j.chemosphere.2021.130881.
Peng, S.-M., Luo, H.-C., Wang, Z.-H., Yang, S.-S., Guo, W.-Q., Ren, N.-Q., 2023. Enhanced in-situ sludge reduction of the side-stream process via employing micro-aerobic approach in both mainstream and side-stream. Bioresour. Technol. 377, 128914. https://doi.org/10.1016/j.biortech.2023.128914.
Semblante, G.U., Hai, F.I., Bustamante, H., Price, W.E., Nghiem, L.D., 2016b. Effects of sludge retention time on oxic-settling-anoxic process performance: biosolids reduction and dewatering properties. Bioresour. Technol. 218, 1187–1194. https://doi.org/10.1016/j.biortech.2016.07.061.
Semblante, G.U., Hai, F.I., Bustamante, H., Guevara, N., Price, W.E., Nghiem, L.D., 2016a. Biosolids reduction by the oxic-settling-anoxic process: impact of sludge interchange rate. Bioresour. Technol. 210, 167–173. https://doi.org/10.1016/j.biortech.2016.01.010.
Semblante, G.U., Hai, F.I., Ngo, H.H., Guo, W., You, S.-J., Price, W.E., Nghiem, L.D., 2014. Sludge cycling between aerobic, anoxic and anaerobic regimes to reduce sludge production during wastewater treatment: performance, mechanisms, and implications. Bioresour. Technol. 155, 395–409. https://doi.org/10.1016/j.biortech.2014.01.029.
Semblante, G.U., Phan, H.V., Hai, F.I., Xu, Z.-Q., Price, W.E., Nghiem, L.D., 2017. The role of microbial diversity and composition in minimizing sludge production in the oxic-settling-anoxic process. Sci. Total. Environ. 607–608, 558–567. https://doi.org/10.1016/j.scitotenv.2017.06.253.
STOWA, 2024. Onderzoek naar het voorspellen van de ontwaterbaarheid van slib en PE gebruik (Report 2024-23). Amersfoort.
Sun, X., Liu, B., Zhang, L., Aketagawa, K., Xue, B., Ren, Y., Bai, J., Zhan, Y., Chen, S., Dong, B., 2022. Partial ozonation of returned sludge via high-concentration ozone to reduce excess sludge production: a pilot study. Sci. Total. Environ. 807, 150773. https://doi.org/10.1016/j.scitotenv.2021.150773.
Sun, H., Zhang, X., Zhang, F., Yang, H., Lu, J., Ge, S., Li, X., Zhang, W., 2021. Tetrasphaera, rather than Candidatus Accumulibacter as performance indicator of free ammonia inhibition during the enhanced biological phosphorus removal processes. J. Environ. Chem. Eng. 9, 106219. https://doi.org/10.1016/j.jece.2021.106219.
Velho, V.F., Foladori, P., Andreottola, G., Costa, R.H.R., 2016. Anaerobic side-stream reactor for excess sludge reduction: 5-year management of a full-scale plant. J. Environ. Manag. 177, 223–230. https://doi.org/10.1016/j.jenvman.2016.04.020.
Wang, X., Wang, S., Xue, T., Li, B., Dai, X., Peng, Y., 2015. Treating low carbon/nitrogen (C/N) wastewater in simultaneous nitrification-endogenous denitrification and phosphorous removal (SNDPR) systems by strengthening anaerobic intracellular carbon storage. Water Res. 77, 191–200. https://doi.org/10.1016/j.watres.2015.03.019.
Wang, K., Zhou, Z., Zheng, Y., Jiang, J., Huang, J., Qiang, J., An, Y., Jiang, L., Jiang, L.-M., Wang, Z., 2020. Understanding mechanisms of sludge in situ reduction in anaerobic side-stream reactor coupled membrane bioreactors packed with carriers at different filling fractions. Bioresour. Technol. 316, 123925. https://doi.org/10.1016/j.biortech.2020.123925.
Xu, S., Yao, J., Ainiwaer, M., Hong, Y., Zhang, Y., 2018. Analysis of bacterial community structure of activated sludge from wastewater treatment plants in winter. Biomed. Res. Int. 2018, 1–8. https://doi.org/10.1155/2018/8278970.
Ye, F., Zhu, R., Li, Y., 2008. Effect of sludge retention time in sludge holding tank on excess sludge production in the oxic-settling-anoxic (OSA) activated sludge process. J. Chem. Technol. Biotechnol. 83, 109–114. https://doi.org/10.1002/jctb.1781.
Zhang, C., Guisasola, A., Oehmen, A., Baeza, J.A., 2023. Benefits and drawbacks of integrating a side-stream sludge fermenter into an A2O system under limited COD conditions. Chem. Eng. J. 468, 143700. https://doi.org/10.1016/j.cej.2023.143700.
Zhang, Y., Qiu, X., Luo, J., Li, H., How, S.-W., Wu, D., He, J., Cheng, Z., Gao, Y., Lu, H., 2024. A review of the phosphorus removal of polyphosphate-accumulating organisms in natural and engineered systems. Sci. Total. Environ. 912, 169103. https://doi.org/10.1016/j.scitotenv.2023.169103.
Zhao, X., Jiang, J., Zhou, Z., Zheng, Y., Shao, Y., Zuo, Y., Ren, Y., An, Y., 2021. Responses of microbial structures, functions and metabolic pathways for nitrogen removal to different hydraulic retention times in anaerobic side-stream reactor coupled membrane bioreactors. Bioresour. Technol. 329, 124903. https://doi.org/10.1016/j.biortech.2021.124903.
Zhao, A., Sun, J., Liu, Y., 2023. Understanding bacterial biofilms: from definition to treatment strategies. Front. Cell. Infect. Microbiol. 13. https://doi.org/10.3389/fcimb.2023.1137947.
Zhou, Z., Qiao, W., Xing, C., Wang, C., Jiang, L.-M., Gu, Y., Wang, L., 2015. Characterization of dissolved organic matter in the anoxic–oxic-settling-anaerobic sludge reduction process. Chem. Eng. J. 259, 357–363. https://doi.org/10.1016/j.cej.2014.07.129.
Zou, X., Lu, Y., Liu, Y., 2025. Divergences of granules and flocs microbial communities and contributions to nitrogen removal under varied carbon to nitrogen ratios. Bioresour. Technol. 425, 132226. https://doi.org/10.1016/j.biortech.2025.132226.